The 33rd Annual Conference of the IEEE Industrial Electronics Society (IECON)
Nov. 5-8, 2007, Taipei, Taiwan

Analytical Comparison Between Ferrite Core and Steel Laminations Losses of Multi-Polar Brushless DC Motor

Wen-Shyue Chen[1, 2] , Chang-Shien Lin[3] and Chern-Lin Chen[4]
[1]Department of Electrical Engineering, National Taiwan University, Taipei, Taiwan
[2]Department of Electrical Engineering, National Taipei University of Technology, Taipei, Taiwan
[3]Department of Electrical Engineering, Northern Taiwan Institute of Science and Technology, Taipei, Taiwan
[4]Department of Electrical Engineering and Graduate Institute of Electronics Engineering, National Taiwan University, Taipei, Taiwan
wschen@ntut.edu.tw, cslin@ieee.org and clchen@cc.ee.ntu.edu.tw

Abstract-**This paper presents an analysis of the stator core losses in two kinds of 3-phase 32-pole brushless DC motors. One stator is manufactured by ferrite and the other is steel laminations. The losses are evaluated by performing time-stepped finite-element analysis and the results are used to evaluate the suitability of the models. The theoretical analysis and experimental results derived from the inverter-controlled BLDC motor drives are presented for confirmation. Experimental results show that the motor with ferrite stator has higher maximum speed and efficiency than those of steel laminations. On the other hand, the motor with steel laminations produces higher torque than that of ferrite material. Based upon these comparison results, ferrite core stator is very promising for low-torque and high-speed applications.**

I. INTRODUCTION

Brushless DC motors, which have higher efficiency than induction or brush DC motors, are now widely used in home appliances [1], industrial machines and electrical vehicles [2, 3]. Compared with DC motors, BLDC motor has no carbon brushes which need to be changed frequently. Also with induction motors, the efficiency of BLDC is much higher. Electronic inverters drive BLDC motors at wide speed ranges with the vector or direct-torque control techniques [4-7]. The operating frequency of BLDC motors increases from 50~60Hz to a few hundred Hz for the purpose of miniaturization and higher power density. In recent motor design, for example, the washing machines, they often use a multi-polar direct-driven motor to take the place of the need for gear boxes [8-10].

Recently, power electronics applications widely proliferate. The high-frequency switching techniques in power electronics open up possibilities to apply the high-frequency magnetic core, ferrite, into not only industries but also home appliances. For this reason, it is interesting for engineers to use the ferrite material as the stator of the BLDC motor.

Due to the developments of power electronics devices, the switching frequency for power converter and lighting apparatus moves from several kilo Hz to hundred kilo Hz, and even MHz. These developments bring the potential applications of high operating frequency to home-appliance motors in which volume is one of main design concerns. To reduce the motor size while not giving negative impact on efficiency motivates this study. Ferrite material has been widely applied to magnetic components for high frequency applications [11, 12].

This paper presents the design considerations, magnetic field analysis of stator and implementation of two 3-phase 32-pole BLDC motors. First, the computer-aided design and analysis are presented, then followed by theoretical analysis and experimental results derived from the inverter-controlled BLDC motor drives are shown. Finally the comparison of the special features of two kinds of BLDC motors in torque and efficiency are presented.

II. DESIGN SPECIFICATIONS AND SIMULATION

In order to accurately compare the torque and loss of the two motors with different soft magnetic materials, four conditions for motor design and test as follows are considered.

1) The same size and shape of the two stators.
2) The type and turn number of stator windings are the same to give the same resistance and inductance, theoretically.
3) The rotor and other mechanical components such as bearings are the same.
4) The test bench, including inverters and load are the same.

As shown in Fig. 1, the test bench consists of a three-phase inverter, designed brushless DC motors [13-15], and PWM commutation circuit.

Table 1 shows the specifications of the designed motor. A ferrite stator and steel laminations are used for stator cores of these two motors, respectively. The rotor has 32 multi-polar Neodymium-Iron-Boron (NdFeB) surface-permanent magnets (SPM) and stator has 24 slots as shown in Fig. 2.

Table 2 shows the related parameters of stator. As shown in Table 2, the size of stator and number of windings for two motors are the same. The ferrite core provides lower

permeability to give lower hysteresis loss as compared to steel laminated core.

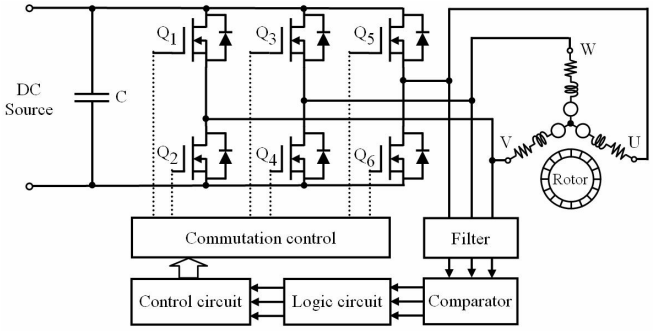

Fig. 1 Circuit diagram of the presented motor driver

Table 1 Motor specifications

Parameter	
Output power (W)	60
Line voltage (V)	9
Line current (A)	8
Stator/phase inductance (μH)	17.6
Stator/phase resistance (Ω)	0.09
No. of phase	3
Connection	Y

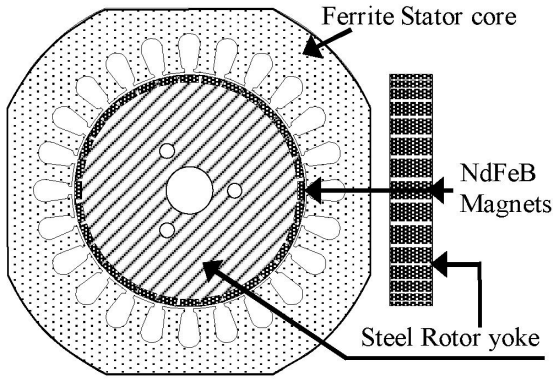

Fig. 2 Cross section of rotor and stator of the presented BLDC motors

To verify the magnetic flux distribution and understand the features of designed motors, computer aided simulation using Finite Element Analysis (FEA) [16] software is used. The simulation results provide magnetic field analysis and thereby adjusting the elements of core to meet the specifications shown in Table 2. The magnetic flux distributions for these two stators are shown in Fig. 3.

As shown in Fig. 3, the designed motor with ferrite core provides lower magnetic flux density as shown in Fig. 3 (a) as compared to that with steel laminations shown in Fig. 3 (b). These simulation results will confirm the experimental results shown later in this paper. Therefore, the designed motor with the ferrite stator has less loss, especially for high operating frequency applications. The disadvantage associated with the reduction of flux density is the torque reduction. These special features will provide a reference for the selection of motor applications.

The iron loss caused by eddy and hysteresis currents can be analyzed [17, 18] by applying Fourier analysis or partial differential equations [19, 20]. However, it is very complex and may not give a whole picture related to motor

Table 2 Parameters of the stator cores

	Ferrite material	Steel laminations
Number of poles	32	32
Number of stator slots	24	24
Permeability	2000	7000
Saturation flux density (mT)	SN-20: Bs = 260	H60: Bs = 1700
Iron loss (W/kg)	165 (at 0.2 T, 100 kHz)	16.5 (at 1.5 T, 60 Hz)
Rotor outer diameter (mm)	64.8	64.8
Stator inner diameter (mm)	64	64
Stator outer diameter (mm)	110	110
Core length (mm)	13	15
Air-gap (mm)	0.4	0.4
Series turns/phase	320 turns	320 turns

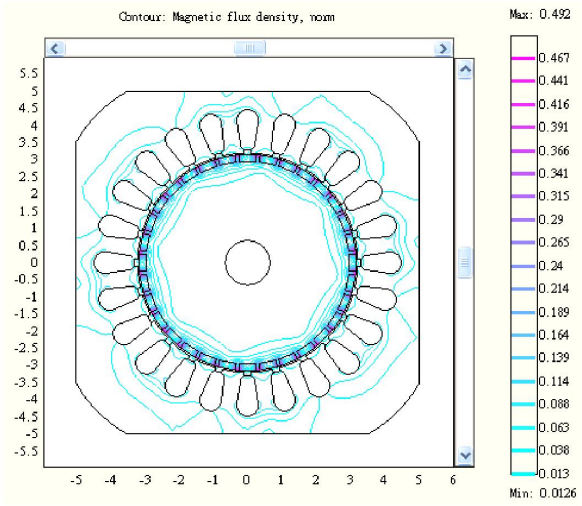

(a) The ferrite stator

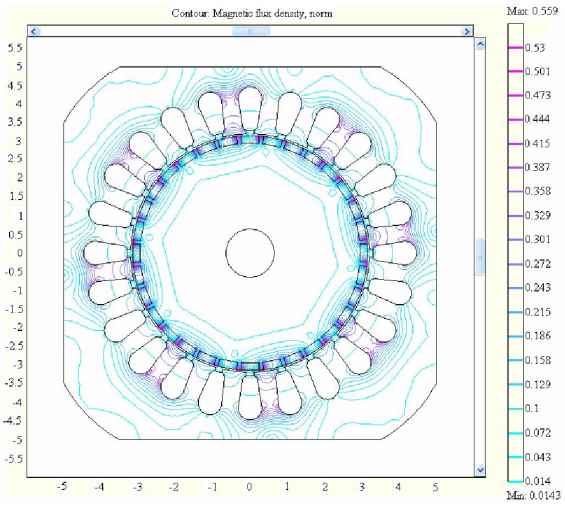

(b) The steel laminated stator

Fig. 3 The magnetic flux distribution of finite-element flux plot for the designed motors

geometry. An alternative way for iron loss analysis is by computer-aided analysis. Fig. 4 shows the iron loss density for the designed motors with ferrite and steel laminated stators. The simulation results are derived using Finite Element Analysis software, named -*MagneForce* [21].

Noting that lighter color gives higher iron loss density. Moreover, the scale of color bar shown in Fig. 4 (a) for the stator with ferrite core is one sixths of that that shown in Fig. 4 (b) for the stator with steel laminations. These simulation results confirm that the designed motor with ferrite stator reduces the iron losses significantly.

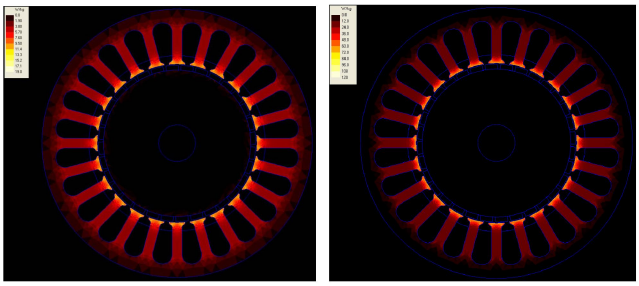

(a) The ferrite stator (b) The steel laminated stator

Fig. 4 Iron loss density of FEA simulation for the presented motor at 2700rpm

III. LOSS ANALYSIS OF THE MULTI-POLAR BLDC MOTORS

To investigate the efficiency of the designed BLDC motors with ferrite and steel laminated stators, motor losses are analyzed as follows. The output power of the motor is [22]:

$$P_{out} = P_{in} - P_{mech} - P_{Cu} - P_{iron} \quad (1)$$

where P_{in} is the input power;
P_{mech} is the mechanical loss;
P_{cu} is the copper loss;
P_{iron} is the iron loss.

If the motors under test have no cooling fans and the bearing loss is trivial as compared to the others, then the mechanical loss can be ignored and the equation shown in (1) can be simplified as:

$$P_{out} \cong P_{in} - P_{Cu} - P_{iron} \quad (2)$$

The copper loss is given by:

$$P_{Cu} = 3R_S i_S^{\,2} \quad (3)$$

where R_s is the stator resistance;
i_s is the stator current.

The iron losses including eddy current loss and hysteresis loss therefore can be represented by:

$$P_{iron} = P_{eddy} + P_{hys} \quad (4)$$

The eddy current loss of the motor is a nonlinear equation as shown in (5) which depends on the frequency, f, and maximum flux density, B_m.

$$P_{eddy} = K_e f^2 B_m^{\,2} t_n^{\,2} \quad (5)$$

where t_n is the thickness of core laminations;
K_e is the eddy loss constant.

The hysteresis loss can be expressed as:

$$P_{hys} = K_h f B_m^{\,n} \quad (6)$$

where n is the Steinmetz constant, which varies from 1.5 to 2 and K_h is the hysteresis loss constant.

The eddy current loss is very small for ferrite core, but rapidly increases with frequency for steel laminations. So the iron loss of the ferrite material can be simplified to be:

$$P_{iron(ferrite)} \cong K_{h(frrite)} f B_m^{\,2} \quad (7)$$

where the iron loss of the steel laminations is:

$$P_{iron(steel)} = K_{e(steel)} f^2 B_m^{\,2} t_n^{\,2} + K_{h(steel)} f B_m^2 \quad (8)$$

IV. TORQUE ANALYSIS OF THE MULTI-POLAR BLDC MOTORS

The torque produced by the designed multi-polar BLDC motor is shown in Fig. 5. Fig. 5 represents its stator and rotor for one electrical angle cycle. The instantaneous force of one stator slot winding is:

$$F = N_p i L \times b \quad (9)$$

where N_p is number of turns per stator pole;
i is the instantaneous current of the stator winding;
L is the effective length of the stator conductor;
b is the induced instantaneous flux density by its rotor permanent magnets.

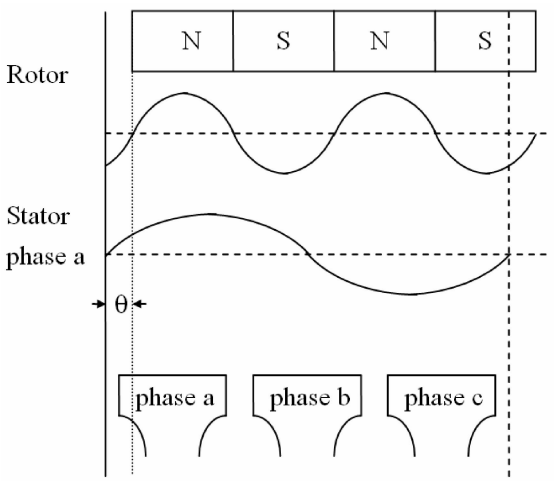

Fig. 5 Flux-density distribution of stator and rotor for one electrical angle cycle

Since one pole has two winding sides, the output force for phase "a" of the motor with P poles is:

$$F_a = 2NiL \times b \quad (10)$$

where N is the total number of turns per phase winding.

By assuming that the current of the stator current i is sinusoidal, the current is expressed by:

$$i = I_m \sin(\omega t) \quad (11)$$

where I_m is the maximum current of stator winding.

The induced flux density b is also sinusoidal and it can be

expressed as:

$$b = B_m \sin(\omega t) \tag{12}$$

where B_m is the maximum flux density induced by the rotor.

The induced voltage, e, determined by Faraday-Lenz's Law is:

$$e = N\frac{d\phi}{dt} = \omega N B_m A \cos(\omega t) \tag{13}$$

where A is the cross section area of the rotor;
ϕ is the flux distribution.

Its instantaneous torque of one pole is:

$$t_p = F_p \times r \tag{14}$$

where r is the radius of rotor.

From Fig. 5, for a three-phase motor, its output torque is:

$$T = t_a + t_b + t_c \tag{15}$$

$$t_a = F_a \times r = 2NLI_m r \sin(\omega t) B_m \sin(\omega t + \theta) \tag{16}$$

$$t_b = F_b \times r = 2NLI_m r \sin(\omega t + 120°) B_m \sin(\omega t + \theta + 240°) \tag{17}$$

$$t_c = F_c \times r = 2NLI_m r \sin(\omega t + 240°) B_m \sin(\omega t + \theta + 480°) \tag{18}$$

Therefore,

$$T = -3NLI_m B_m r \cos(\theta) \tag{19}$$

If the angle θ is identified by the Hall sensor or by sensorless circuit such that we can control the rotor to let the rotor flux be in-phase with stator, the maximum torque is:

$$T_m = -\frac{3}{2} N B_m I_m A \tag{20}$$

As shown in (20), because ferrite material has lower flux density than steel laminations, the output torque for the motor with ferrite stator is smaller than that with steel laminated stator.

V. IMPLEMENTATION AND EXPERIMENTAL RESULTS

In order to derive the comparison results two motors with ferrite stator and steel laminated stator are designed and implemented. Their rotors are made of 32-pole NdFeB surface permanent magnets. The schematic of implemented stator windings is shown in Fig. 6(a) and the related three-phase winding distributions are summarized in Fig. 6(b), each phase has eight branches.

The stators of prototype have 16-pole, 3-phase stator windings, as shown in Fig. 7. The stator windings consist of 80-turn AWG#28 wire conductors per slot. As shown in Fig. 7 (a) and Fig. 7 (b), two motors are identical in geometry. The only difference is the material of stator; one

Coil No.	Phase A		Phase B		Phase C	
	In	Out	In	Out	In	Out
1	1	2	2	3	3	1
2	4	5	5	6	6	4
3	7	8	8	9	9	7
4	10	11	11	12	12	10
5	13	14	14	15	15	13
6	16	17	17	18	18	16
7	19	20	20	21	21	19
8	22	23	23	24	24	22

(a) Winding distributions, conductor in and out

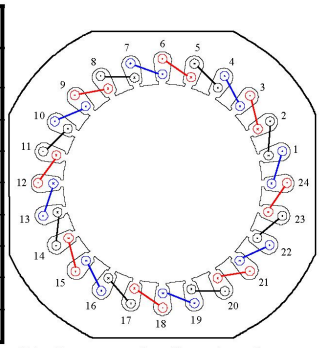

(b) Stator winding in slot

Fig. 6 Schematic of stator windings with 8 branches per phase

consists of ferrite as shown in Fig. 7 (a) and the other one is steel laminations as shown in Fig. 7 (b).

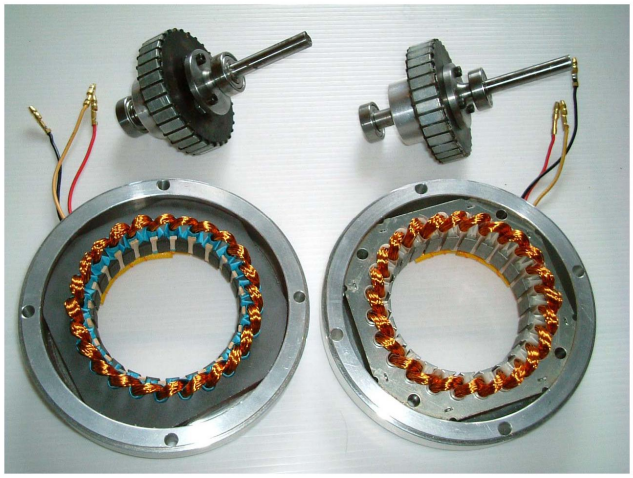

(a) With ferrite stator (b) With steel laminated stator

(c) The assembled BLDC motor

Fig. 7 The prototypes of BLDC motor with stator windings and NdFeB surface permanent magnets (SPM) rotor

The testing system consists of a computer and sensors to measure the torque, speed and power of the motors. A 3-phase sensorless SPWM ac driver operates the two motors from 900 to 3000rpm. Output power of two motors at different speed is recorded and listed in Table 4 for the ferrite motor and Table 5 for the steel laminated one. By (20), the output torque of the ferrite motor is 0.14 N-m ≒ 1.4 kg-cm when N=320 Turns, B_m=0.25 T, I_m=1.414 A and A=0.064m×0.013m. The output torques vs. speed is shown in Fig. 8. It is shown that the maximum torque for the motor

with ferrite stator is 1.5 kg-cm and torque for the motor with steel laminated stator can exceed 3.0 kg-cm. In Table 4, Table 5 and Fig. 8, for the purpose of comparison, we only show the same range of torque and speed.

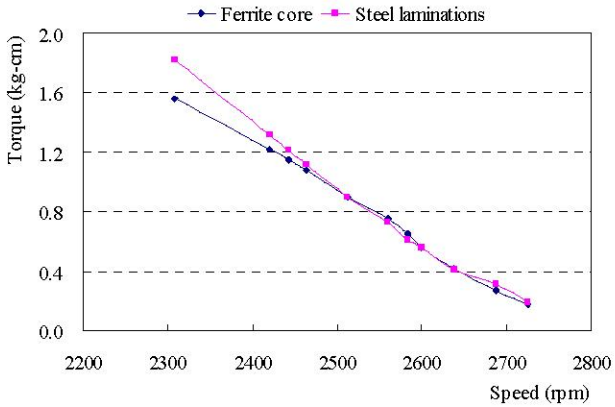

Fig. 8 Output torques vs. speed

Table 4 Output power of the motor with ferrite stator

Motor speed (rpm)	Output power (W)	Efficiency (%)
2292	36.68	61.08
2372	31.88	64.17
2412	30.19	66.05
2446	28.86	68.24
2468	26.33	70.85
2512	23.20	69.61
2560	21.01	66.45
2586	17.25	65.40
2606	14.97	62.93
2640	11.38	58.07
2694	7.46	49.65
2704	4.99	44.31

Table5 Output power of the motor with steel laminated stator

Motor speed (rpm)	Output power (W)	Efficiency (%)
2368	36.93	60.90
2394	35.12	59.75
2420	32.77	58.77
2443	30.33	56.86
2464	28.31	55.40
2478	26.95	53.94
2512	23.20	50.33
2523	21.49	48.31
2560	19.17	44.80
2584	16.17	41.57
2600	14.94	39.28
2638	11.10	32.84
2688	8.55	25.64
2725	5.31	17.42

In Fig. 9, we compare the efficiency of these two motors. The efficiency for the ferrite motor is higher than steel laminated one in the whole speed range and under all load conditions. The maximum efficiency of the ferrite motor is 70.85%. Less than 1.5 kg-cm load, the maximum efficiency of steel laminated motor is 60.9% while 61.08% for the ferrite motor. Moreover, the maximum speed of the ferrite motor is about 5800 rpm which is higher than that of 2700 rpm for steel laminated one when input voltage is 12 VDC. Its torque-speed curves at high speed region are shown in Fig. 10. Its maximum efficiency is 76.89% at about 4900 rpm.

In addition, we made no-load tests for two prototypes. The input power vs. speed is shown in Fig. 11. The input power for the motor with steel laminated stator is much higher than that of the ferrite motor for higher iron losses caused by eddy current loss and hysteresis loss. This result is consistent with that derived from simulation as shown in Section 3.

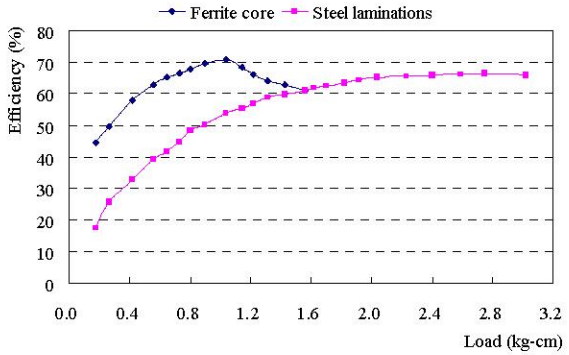

Fig. 9 Efficiency vs. load of the different stator material for the presented motor

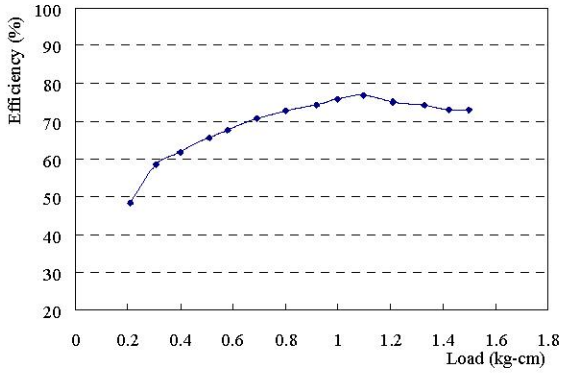

Fig. 10 Efficiency vs. load of the ferrite material at high speed

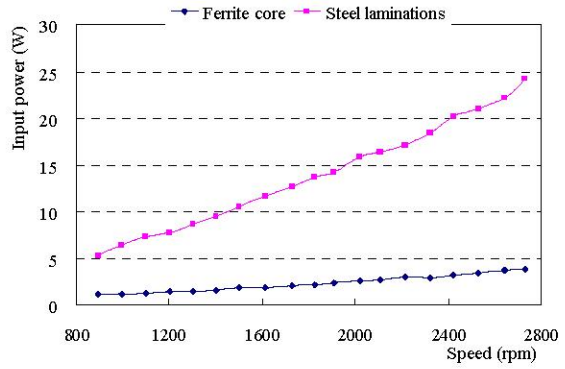

Fig. 11 Input power vs. speed of the different stator material for the presented motor

VI. DISCUSSION AND CONCLUSIONS

In this paper, comparative study on the two types of brushless DC motors is performed. These BLDC motors with identical geometry and specifications are designed and implemented. By computer-aided design and experimental results derived from the inverter-controlled BLDC motor drives, some remarks are made as follows:

1) The motor with ferrite stator is promising for high frequency motor drives applications due to lower iron losses. The experimental results show that the motor with ferrite stator provides 15 % efficiency advantages over the other one with steel laminated stator at torque less than 1 kg-cm.

2) For the same DC-link voltage of inverter, the maximum speed range for the motor with ferrite stator is much higher than that of the motor with steel laminated stator. This special feature is contributed by lower flux level. The disadvantage related to lower flux level is the reduction of maximum torque.

In short, the motors with ferrite stator have higher maximum speed and efficiency than those of steel laminations. On the other hand, the motor with steel laminated stator produces higher torque than that of ferrite material. Based upon these comparison results, the motor with ferrite stator is very promising for low-torque and high-speed applications.

ACKNOWLEDGMENT

This work was supported by the National Science Council of Taiwan, Republic of China, under grant contract NSC 94-2213-E-149-008.

REFERENCES

[1] A. Barkley, D. Michaud, E. Santi, A. Monti, and D. Patterson, "Single Stage Brushless DC Motor Drive with High Input Power Factor for Single Phase Applications,". *Proc. IEEE PESC*, pp. 1–10, 2006.

[2] C.H. Chen, and M.Y. Cheng, "A New Sensorless Commutation Drive for Brushless DC Motors and Alternators," *Proc. IEEE IECON*, vol. 3, pp. 2116–2121, 2006.

[3] C.H. Chen, and M.Y. Cheng, "Design of a multispeed winding for a brushless dc motor and its sensorless control," *IEE Proc., Electr. Power Appl.*, vol. 153, pp. 834–841 2006.

[4] I. Takahashi, and T. Noguchi, "A new quick-response and high-efficiency control strategy of an induction motor," *IEEE Trans. Ind. Appl.*, vol. 22, pp. 820–827, 1986.

[5] M. Depenbrock, "Direct self-control (DSC) of inverter-fed induction machine," *IEEE Trans Power Electron.*, vol. 3, pp. 420–429, 1988.

[6] T.G. Habetler, F. Profumo, M. Pastorelli, and L.M. Tolbert, "Direct Torque Control of Induction Machines Using Space Vector Modulation," *IEEE Trans. Ind. Appl.*, vol. 28, pp. 1045–1053, 1992.

[7] Y. Liu, Z.Q. Zhu, and D. Howe, "Instantaneous Torque Estimation in Sensorless Direct-Torque-Controlled Brushless DC Motors," *IEEE Trans. Ind. Appl.*, vol. 42, pp. 1275–1283, 2006.

[8] L.O. Hultman, and A.G. Jack, "Soft Magnetic Composites – Materials and Applications," *IEEE IEMDC*, pp. 516-522, 2003.

[9] A.G. Jack, B.C. Mecrow, G. Nord and P.G. Dickinson, "Axial Flux Motors Using Compacted Insulated Iron Powder and Laminations –Design and Test Results," *IEEE IEMDC*, pp. 378-385, 2005.

[10] U.S. Deshpande, "Recent Advances in Materials for use in Permanent Magnet Machines – A Review," *IEEE IEMDC*, pp. 509-515, 2003.

[11] C.K. Liu, T.W. Law, P.L. Cheng, I.T. Chong and D.C.C. Lam, "Low temperature processing and electrical properties of embedded ferrite-cored inductor," *Proc. IEEE ECTC*, pp. 490–494, 2002.

[12] A.R.A. Razak, and S. Taib, "Design considerations of a high frequency power transformer," *Proc. IEEE PECON*, pp. 243–248, 2003.

[13] N. Bianchi, S. Bolognani, "Brushless DC motor design: an optimisation procedure based on genetic algorithms," *IEE EMD97*, no. 444, pp. 16–20, 1997.

[14] N. Bianchi, S. Bolognani, F. Luise, "Analysis and Design of a PM Brushless Motor for High-Speed Operations," *IEEE Trans. Energy Conv.*, vol. 20, no. 3, pp. 629–637, 2005.

[15] N. Bianchi, S. Bolognani, P. Frare, "Design criteria for high-efficiency SPM synchronous motors," *IEEE Trans. Energy Conv.*, vol. 21, no. 2, pp. 396–404, 2006.

[16] A. Daikoku, M. Nakano, S. Yamaguchi, Y. Tani, Y. Toide, H. Arita, T. Yoshioka and C. Fujino, "A high precision motor design method by finite element analysis considering stress distribution in stator core," *IEEE IEMDC*, pp. 366–372, 2005.

[17] C.T. Mi, G.R. Slemon, and R. Bonert, "Modeling of iron losses of permanent-magnet synchronous motors," *IEEE Trans. Ind. Appl.*, vol. 39, pp. 734–742, 2003.

[18] K. Yamazaki, and Y. Seto, "Iron loss analysis of interior permanent-magnet synchronous motors-variation of main loss factors due to driving condition," *IEEE Trans. Ind. Appl.*, vol. 42, pp. 1045–1052, 2006.

[19] D. Fang, and T.W. Nehl, "Analytical modeling of eddy-current losses caused by pulse-width-modulation switching in permanent-magnet brushless direct-current motors," *IEEE Trans. Magn.*, vol. 34, pp.3728–3736, 1998.

[20] X.H. Wang, Q.F. Li, S.H. Wang, and Q.H. Li, "Analytical calculation of air-gap magnetic field distribution and instantaneous characteristics of brushless DC motors," *IEEE Trans. Energy Conv.*, vol. 18, pp. 424–432, 2003.

[21] *Brushless DC motor and Induction motor User's Guide*. The MagneForce Software systems Inc. Hamburg, NY

[22] M.E. El-Hawary, "Principles of electric machines with power electronic applications," (Piscataway, NJ, IEEE Press, 2002, 2nd edn.)